Sensors and Actuators B 237 (2016) 776–786

Contents lists available at ScienceDirect

Sensors and Actuators B: Chemical

journal homepage: www.elsevier.com/locate/snb

Design and fabrication of capacitive nanosensor based on MOF nanoparticles as sensing layer for VOCs detection

S. Homayoonnia, S. Zeinali*

Department of Nanochemical Engineering, Faculty of Advanced Technologies, Shiraz University, Shiraz, Iran

ARTICLE INFO

Article history:
Received 26 November 2015
Received in revised form 25 June 2016
Accepted 27 June 2016
Available online 28 June 2016

Keywords:
Chemical gas sensor
Capacitive sensor
VOCs
MOF
Cu-BTC nanoparticles

ABSTRACT

Due to high porosity and increased surface area; metal organic frameworks (MOFs) have been widely used in gas storage applications as well as volatile organic compounds (VOCs) detection. Most of these sensors are electromechanical or electrochemical based; however there are few works in which capacitive sensors were developed using micrometer MOFs. In the present study, for the first time, MOF (Cu-BTC) nanoparticles were used to develop capacitive sensor device for detecting VOCs (e.g. methanol, ethanol, isopropanol, and acetone). The studied capacitive sensors were performed in a moderate environment (10% relative humidity and 25 °C). Capacitive sensors were fabricated in a sandwich form or parallel plate by using copper plate as a back electrode, MOF nanoparticles layer as the dielectric, and interconnected silver spots as the upper electrode of the capacitor. Linearity of the response versus LCR meter frequency, reusability, reversibility, response time, and limit of detection (LOD) of the capacitive sensor were determined to evaluate the sensor performance. The results showed high ability of Cu-BTC nanoparticles synthesized as dielectric layer of a capacitive nanosensor to determine VOCs.

1. Introduction

Chemical gas sensors find extensive applications in toxic and combustible gas monitoring, automobile combustion control, medical analysis, and energy and drying operations markets. The emerging markets include defense, consumer products, automobiles, wastewater treatment, food, beverage processing, etc. In contrast to the conventional equipment for gas separation and detection such as gas chromatography, ion mobility spectroscopy, and mass spectroscopy; gas sensors are more cost effective and have simpler instrumentational operation especially for real-time and in situ applications [1]. Interaction of the analyte vapor with the sensing layer of a chemical gas sensor leads to physical parameter changes such currents, electrical conductance, capacitance, absorbance, mass or acoustic variables which are all correlated to the analyte concentrations. Interactions between the analytes and sensing materials are multiform, depending on the analytes and active materials [2].

Volatile organic compounds (VOCs) are one of the most popular gases whose detections are highly desirable. There is consequently a surge of interest in the development of s VOCs sensors because they constantly risk our wellbeing as well as the environment around us and cause chronic health threats to human beings, animals and plants. Volatile organic compounds also contribute to climate change and destruction of the ozone layer [3,4]. The low flashpoints of VOCs makes them particularly threatening in closed areas.

Metal organic frameworks (MOFs) constitute a new generation mesoporous crystalline materials, which are composed of both organic and inorganic components in a rigid periodic networked structure [5]. MOFs are currently attracting considerable attention as ideal candidate for sensing material because of their non-toxic nature, tailorable nanoporosity, extraordinary regularity of their porosity, ultrahigh surface areas, reversible sorption characteristics and analyte specific adsorption [6,7]. In addition, MOFs are often reversible allowing for time durable devices [8]. To date various types of MOFs have been used as sensing materials in electromechanical devices including surface-acoustic wave (SAW) sensors [9], quartz crystal microbalances (QCMs) [10,11], microcantilevers [12–14], and electrochemical devices including capacitors [15] and impedance sensor [16] mainly for VOCs and humidity. Cu-BTC (also known as HKUST-1), with chemical formula of Cu_3 $(BTC)_2$, is a well investigated MOF both theoretically and experimentally. It consists of Cu ions and benzene tricarboxylate (BTC) as a linker [17].

Gas adsorption on the materials surfaces are significantly affected by the temperature and relative humidity. Therefore, it

* Corresponding author.
E-mail addresses: zeinali@shirazu.ac.ir, zzeinali@yahoo.com (S. Zeinali).

http://dx.doi.org/10.1016/j.snb.2016.06.152
0925-4005/

is crucial to investigate the gas sensing performance under "real-world" conditions. There are some reports in which the surface degradation and structural alteration of the Cu-BTC framework were studied after being exposed to the moist air for a period of days [18–22]. The majority of studies and simulations on Cu-BTC based sensor occur under idealized conditions (for example, gas adsorption in dry nitrogen or Cu-BTC storage at elevated temperatures or under nitrogen flow prior to usage) which are not appropriate for a real world application [23]. On the other hand, according to Kusgens et al. [18], the water stability of Cu-BTC might be sufficient for molecular recognition if the framework is not directly exposed to liquid water. Hence, this shows the advantage of using Cu-BTC as a sensing layer particularly at ambient conditions. Moreover, the recent work by Davydovskaya et al. [23] demonstrates that Cu-BTC based QCM sensor's response to VOCs is different under different humidity levels, and at lower humidity levels (below 20%), the relative order during exposure to different alcohol vapors was unchanged in comparison with dry air. Thus, further investigations as a function of the working environment of the sensor are required for the signal intensities.

Generally, the capacitive type sensors are more popular because they use less power, low cost and have the advantage of miniaturization, ease of signal treatment, simplicity of structure, high sensitivity, good reproducibility, quick response and much better linearity. The key advantage of a capacitive-type sensor is its selective detection of the specific gas molecules [24,25]. Since most of MOFs are insulating materials, they can play important role as dielectric layer of the capacitors. Although this potential is often noted, to date there are few reports on MOFs which were used as a key component of a capacitive sensor, in which mostly micrometer scaled MOFs particles were used.

Recently, nanometer materials such as nano-crystalline SnO_2/TiO_2 bilayered films, ZnO nanorods, carbon nanotube films, Pt/graphene nano-sheets, niobium tungsten oxide nanorods, and carbon nanotubes have received great attention for their higher sensitivity due to their small grain size and large surface area [26–31]. The reduction of MOF crystal size to the nanometer scale results in a dramatic decrease in diffusion length and an increase in accessible active sites as compared to the bulk counterparts. These parameters in turn lead to improvement of the adsorption as well as more efficient gas sensing performance and high sensitivity of MOF nanoparticles [32,33].

Some common methods such as directed self-assembly, layer-by-layer deposition, and drop casting were carried out in order to fabricate the sensing material layers. The drop-casting method is usually considered as an unsuitable choice to obtain homogeneous crystalline layers with a controlled thickness [34], and hardly controls the uniformity of the layers on the substrate, but usually resulting in the 'coffee-ring' effect. Drop casting does serve a quick, low cost and accessible method to generating thin layers on relatively small substrates and with assistance of some proper strategies, uniform and controllable layers can be produced by drop casting method [35–43]. In addition, this method is not limited to the substrate material and the thickness of the layer can be controlled by level of drop concentration and number of drop-casting cycles [34].

In this work, the active sensing layer is made from Cu-BTC (HKUST-1) nanoparticles which were used as dielectric layer of parallel-plate capacitors. These capacitive sensors were fabricated at room temperature using drop casting technique for the detection of different concentrations of VOCs (e.g., methanol, ethanol, isopropanol, and acetone). In general, the dielectric layer used for parallel-plate capacitance sensor should be thick enough to prevent touching or connecting of two parallel electrodes which can result in a short-circuit. In order to have low capacitance leakage at alternating current which can lead to the capacitors' life-time decreasing, MOF layer should also be crack free and uniform. The successful preparation of well-behaved MOF layer leads to a good sensor property with excellent sensitivity and response time to VOCs as reflected by the measured capacitances. In this work, by using some strategies in drop casting method, a uniform, crack free layer with sufficient thickness were achieved that is appropriate to be used as dielectric layer in a capacitance sensor. To the best of our knowledge, this work is the first report of using MOF in nanoscale for fabricating a parallel plate capacitive gas sensor, and the first report of using Cu-BTC in nanoscale for fabricating a capacitive gas sensor device for VOCs detection at real condition (room temperature and atmospheric humidity).

2. Experimental

2.1. Materials

Copper plates ($2 \times 2 \times 0.002$ cm, >99.90%), 1,3,5-Benzentricarboxylic acid (H_3BTC, 98%), cupric acetate dihydrate ($Cu(OAc)_2.H_2O$), dimethylformamide (DMF), ethanol (99.9%), methanol (100%), isopropanol (≥99.8%), acetone (≥99.8%), were purchased from Merck company and used as received. Ag paste was purchased from an Iranian Company (Hezareh-3 Company, Iran) and used in fabrication of capacitors.

2.2. Apparatus

Ultrasonic synthesis of Cu-BTC was carried out by applying an ultrasonic disruptor (TOMY UD-201). All sensing tests were done by using a home-made sensing chamber. The characterization of MOF layer was performed by SEM imaging (VEGA TS 5136MM), XRD (Bruker D8 Advanced), FTIR spectroscopy (Perkin-Elmer Spectrum RX I) and BET (PHS-1020) data, and a LCR meter (KC-605) was used to measure the capacitance.

2.3. Preparation of Cu-BTC nanoparticles

An exact amount of 1,3,5-benzenetricarboxylic acid (H_3BTC, 0.5 mmol) was dissolved into a solvent mixture of ethanol (2 mL) and DMF (1.0 mL), and then mixed with an aqueous solution (4 mL) of cupric acetate dihydrate (0.5 mmol) in a sample vial and stirred magnetically for 10 min. The vial was set to the probe of an ultrasonic generator (100 W) under the room temperature (around 25 °C). After 1 min ultrasonic irradiation, the product was separated from the reaction mixture by centrifugation and washed with ethanol (8 mL). Stable colloidal suspensions of Cu-BTC were obtained by re-dispersing the washed product in ethanol.

2.4. Fabrication of Cu-BTC layer as dielectric material on copper slide

In this work, a uniform layer was achieved through a modified drop casting method, which could be used as dielectric layer in the capacitive sensor. The solvent, its evaporating time, and the solution concentration are the key factors affecting the uniformity of the films as well as their physical properties [35,36]. Among different solvents that were examined, ethanol was chosen as the best for making a stable suspension of Cu-BTC. According to the evaporating rate of ethanol which is not so fast, a good layer could be obtained. Further, an improvement in drop spreading over the substrate was achieved via combination of tilted-drop casting and weak vibration of substrate during the solvent evaporation. This could result in lower roughness of the deposited layer and more uniform films. Multi layers of a film were deposited sequentially by using the same manufacturing process. The nanoscale particles of Cu-BTC had great

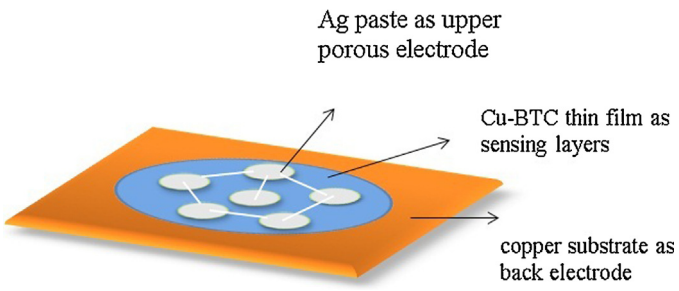

Fig. 1. Schematic of the fabricated capacitive sensor based on the nano Cu-BTC layer.

effect on achieving a homogenous suspension of Cu-BTC nanoparticles in ethanol because of their smaller particles size. This property leads to successful adhesion of nanoparticles to the substrate which consequently influenced in uniformity of the film and resulted in homogenous and crack free film.

In order to investigate the reproducibility of the fabricated sensors, four individual sensors were prepared based on the procedure mentioned above, and their results were compared with each other. The results will bring in future section.

2.5. Fabrication of parallel-plate capacitance sensor

Parallel-plate capacitance sensors [44–48] consist of a metal substrate as back electrode, followed (deposited) by a dielectric layer as sensing material, and a second, porous layer of metal on top of it as upper electrode. In this work, Cu-BTC sensing layers were drop-coated on the copper back electrodes and subsequently dried. The upper porous electrode was made by placing six interconnected drops of Ag paste (2 mm diameter) on the Cu-BTC layer (Fig. 1).

This pattern allows an efficient adsorption and diffusion of target gases in the Cu-BTC dielectric layer. The electrical contacts are made exclusively on the bottom electrode and patterned up electrode using copper wires. Then, the whole device was backed on an oven at 100 °C for 30 min. The prepared capacitive sensors were stored at ambient conditions (25 °C and relative humidity of about 10%) and used for the evaluation of gas sensing without further treatment.

2.6. Characterization methods

Dried Cu-BTC powder was characterized by powder infrared (IR) spectroscopy and BET. The Cu-BTC layer was characterized by X-ray diffraction (XRD) and scanning electron microscopy (SEM). IR spectra were collected by Perkin-Elmer Spectrum RX I spectrometer with an attenuated total reflectance unit. XRD measurements were carried out on a Bruker D8 Advanced device. SEM micrographs were recorded with a VEGA TS 5136MM microscope.

2.7. Sensor test setup (sensing system)

The capacitance (C) of one capacitor is expressed as:

$$C = \varepsilon_0 . \varepsilon_r \frac{A}{d} \quad (1)$$

Depending on the target gas concentration in the atmosphere, one of the parameters, the distance between electrode (d), dielectric constant (ε_r), or area of electrode (A), needs to be changed in a capacitive gas sensor [22]. When the proposed capacitance sensor with nanoporous Cu-BTC dielectric layer is exposed to different target gases, the analyte molecules are adsorbed in Cu-BTC layer through the space between dotted top (upper) electrodes. Because of the mesoporous nature of MOF layer and the fact that their pores are connected together via the intracrystalline channels [49], the analyte molecules can diffuse to everywhere in Cu-BTC layer even to the sandwiched part of Cu-BTC layer between dotted top electrode and down electrode plate. Adsorption of gas molecules in Cu-BTC pores caused a change in capacitance of the sensor. Because of the rigidity of nanoporous Cu-BTC layer, changes in capacitance of the sensor by exposure to analytes is only related to change in dielectric constant of the dielectric material (Cu-BTC) (Eq. (1)). The capacitance sensor's response represents the changes in capacitance (C) that measured by LCR meter.

In this work, some polar VOCs including methanol, ethanol, isopropanol, and acetone were used as target gases. The main characteristics parameters of these selected analytes were shown in Table 1. The sensing process occurred in a home-made chamber contained a Pyrex glass chamber of 2 L volume which was carefully sealed. The fabricated capacitive sensor (Section 2.5) was positioned on a stand in the test chamber where the VOC vapors were produced. A micro heater was put in the chamber for providing vapor of VOC analytes. We used a syringe to inject predetermined volumes of VOC in liquid phase on heater surface to create concentration of 250, 500, 1000 and 1500 ppm of VOCs in the sensing chamber. The method used for calculating VOCs' concentrations was explained in supporting information (Section 1). A fan was also used to make a homogeneous concentration of vapor in the chamber (Fig. 2). Similar sensor set up was reported with others [50,51].

The sensing chamber was exposed to atmospheric air at the beginning in order to have the atmospheric condition in our sensing chamber. To evaporate each analyte, the surface temperature of the microheater was adjusted to its boiling point and we turned it off to prevent increasing the sensing chamber temperature after evaporation of VOCs. Therefore, humidity and temperature of the chamber are equal to atmospheric air conditions during the sensing test (10% relative humidity and 25 °C. Because our system is batch and the sensing chamber was carefully sealed, no considerable change in humidity and temperature was observed.

The variations of the sensor capacitance were measured using a LCR meter during a certain time range within 1 min increments. Linearity of the response versus LCR meter frequency, reusability, reversibility, response time, sensitivity, and limit of detection (LOD) of the capacitive sensor were determined to evaluate the sensor performance.

3. Results and discussion

3.1. Characterization of Cu-BTC sensing layer

3.1.1. FTIR spectroscopy

IR spectroscopy was used to characterize functional groups in samples. The FTIR spectrum of Cu-BTC nanoparticles shows the characteristic asymmetric stretching vibrations of carboxylate groups in the BTC linker at 1650 cm^{-1} and the symmetric stretching vibrations around 1435 and 1375 cm^{-1} (Fig. 3). However, the vibration band in this wavenumber range could also be resulted from stretching vibration of the benzene ring as well as deformation vibration of water molecules. Beside bands related to COO^- groups, the band at 1435 cm^{-1} is ascribed to the C—C vibration in the aromatic ring. Furthermore, the peak at 1105 $cm^{-1}$is assigned to the C—O stretching vibration of primary alcohols. The presence of water molecules is confirmed by a broad band in the region of 3800–2700 cm^{-1} originating from stretching vibration of OH groups from water molecules and the peak around 730 cm^{-1} is related to the bending vibration of C—H. The FTIR absorption band centered at 507 cm^{-1} is due to a vibrational mode involving the Cu center. The results are in good agreement with some other reported

Table 1
Summary of VOCs' properties.

Analyte	Chemical formula	Dielectric constant [65]	Dipole moment (D) [66]	Kinetic diameter (**A**°) [67,68]	Molar mass (g/mol)
Methanol	CH_3-OH	33.00	1.70	3.80	32.04
Ethanol	CH_3-CH_2-OH	24.55	1.69	4.50	46.07
Isopropanol	$CH_3-CH(-OH)-CH_3$	18.00	1.66	4.70	60.10
Acetone	$CH_3-C(=O)-CH_3$	21.00	2.88	4.70	58.08

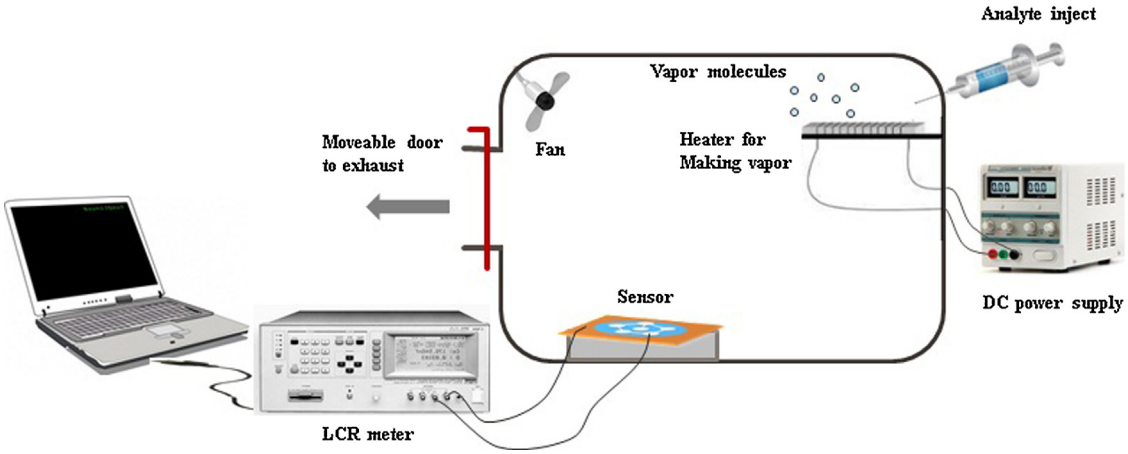

Fig. 2. Schematic of experimental setup for capacitive gas sensing.

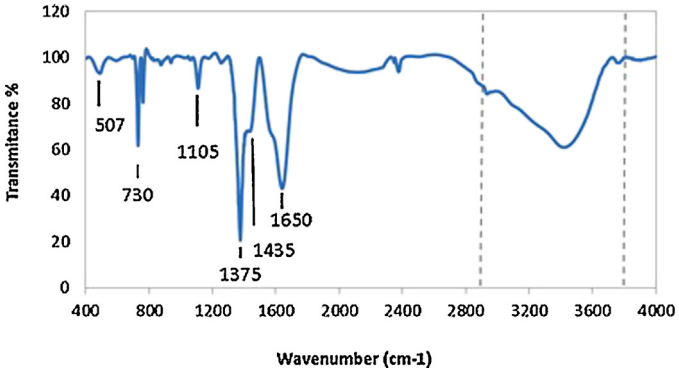

Fig. 3. FTIR spectrum of as-prepared nano Cu-BTC layer.

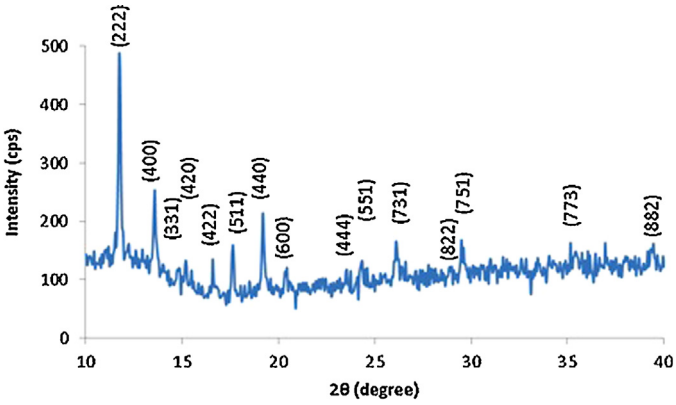

Fig. 4. X-ray diffraction patterns of as-prepared nano Cu-BTC layer.

FTIR spectra for Cu-BTC and confirm that the samples with nanostructure are indeed the Cu-BTC product [52–55].

3.1.2. X-Ray diffraction analysis

The XRD pattern of the as-prepared Cu-BTC layer is shown in Fig. 4. As-prepared Cu-BTC consists of a face-centered cubic (FCC) crystal lattice, with reflections of (222), (400), (331), (420), (422), (511), (440), (600), (444), (551), (731), (822), (751), (773), and (882) planes at 2θ of 11.66, 13.46, 14.3, 15.08, 16.48, 17.48, 19.06, 20.3, 23.05, 24.25, 26.1, 28.35, 29.5, 35.15, and 39.15; respectively. All diffraction peaks match well with the data in the standard pattern, and no obvious peaks of impurities can be detected: indicating that the as-synthesized samples are pure phase of Cu-BTC. The peaks are clear and sharp, which indicate that Cu-BTC sample has good crystallinity. No characteristic reflections of the copper slice were observed, suggesting a good coverage of the support by the Cu-BTC layer [53,56,57].

3.1.3. Scanning electron microscopy (SEM)

The morphologies and particle sizes of as-prepared Cu-BTC layer on the copper slide were investigated by SEM (Fig. 5). The SEM images prove that the film is defect-free, and the Cu-BTC crystals with a size of about 100 nm are merged tightly (agglomerated) with each other.

Agglomeration is a common phenomenon observed in the nanoparticles. Agglomerate is a non-intergrown association of primary particles aligned where the total surface area is slightly different from the sum of the individual surface area [58]. This small decrease of surface area may cause only a small decrease in accessible active sites and increase in diffusion length of analytes which consequently cause a little increase in response time and little decrease in sensitivity of the sensor in detection. But, this agglomeration is desirable for fabricating of thin layer of the capacitance sensor in this work. Because, agglomeration resulted in more particle–particle interaction and consequently formation of crack free and uniform film which cause low capacitance leakage and more life-time of capacitance sensors.

The cross-section image in Fig. 5c illustrates that the crystals anchor compactly and uniformly on the copper support. It can be estimated that the thickness of the Cu-BTC layer is about 8μm.

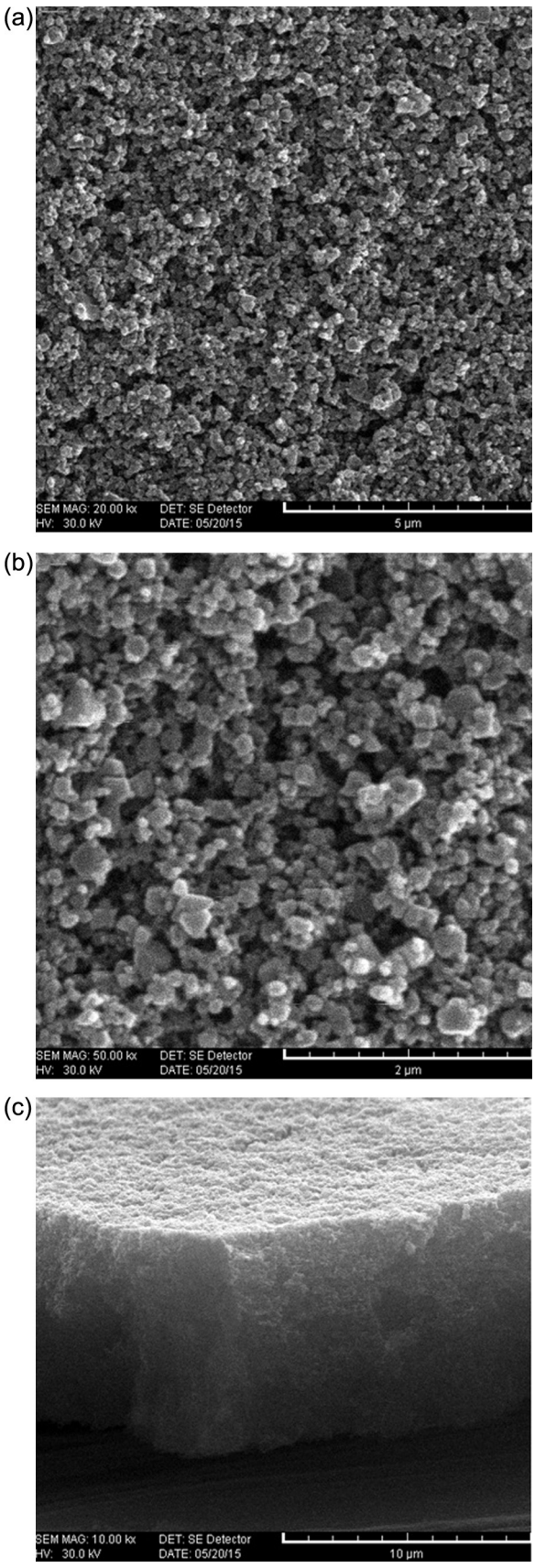

Fig. 5. SEM images of (a) the surface, (b) surface in more magnify view and (c) cross section of the as-prepared nano Cu-BTC layer on the copper slide.

Table 2
Result of BET analysis for Cu-BTC nanoparticles.

Parameter	Value
BET specific surface area	1262.976 m^2/gr
LAN specific surface area	1391.263 m^2/gr
The total Hole Volume	0.467 m^3/gr

3.1.4. BET analysis

In order to study the surface area and pore size of synthesized nano Cu-BTC samples, BET test was done. The results were shown in Table 2. It can be observed that nanoporous material with nanometer particles was obtained with reasonable surface area (1262.976 m^2/gr), which can lead to an increase of the interaction between gaseous molecules and sensing material.

3.2. Sensor performance evaluation

In this study, an archetype capacitor sensor is connected to an alternating current or AC circuit by LCR meter. This capacitor is frequency dependent. Therefore, in order to have the optimum linear relation in our response, capacitance at different frequency of LCR meter was measured under room temperature. We measured the methanol capacitance response under five frequencies 800 Hz, 1 kHz, 10 kHz, 100 kHz, and 1 MHz with methanol concentration of 250, 500, and 1000 ppm (Fig. 6).

According to the calculated R^2 values in Fig. 6, the best linearity was observed at frequency 1 MHz. Similar results were obtained for other analytes detections (the results were not shown here). Therefore, 1 MHz was chosen as the best applied frequency in all experiments.

3.2.1. The effect of variation of Cu-BTC nanoparticle size on the device characteristics and detection process

The size of mesoporous materials is important since it determines the diffusion path through the nanopore space. By decreasing the size of mesoporous materials, a substantial change in their properties is expected [49]. Thus, in order to investigate the effect of Cu-BTC nanoparticles size variation on the detection properties of sensors, two different sizes (S1, with nanoparticle mean diameter = 104.9 nm, and S2, with mean diameter = 168.4 nm) of Cu-BTC nanoparticles were synthesized for using as dielectric layer of two different capacitance sensors. S1 and S2 samples were synthesized according to the procedure explained in Section 2.3 and supporting information (Section 2). Additionally, they were compared to their microsized counterparts (S3, with particle mean diameter = 2 μm) which were prepared in our previous work [51] to investigate the novel properties of nanometer Cu-BTC in comparison to their micronsized counterparts. Fig. 7 shows the time-dependent capacitive responses ($(\Delta C/C_0)$ where $\Delta C = (C_t - C_0)$ is sensor's capacitance changes, and C_0 is sensor's baseline capacitance in the absence of any analyte) of sensors S1, S2, and S3 which were exposed to 500 ppm ethanol at 25 °C and relative humidity of 10%. As expected, the reduction of Cu-BTC nanoparticle size to the nanometer (compared to micrometer) scale leads to more efficient gas sensing performance, faster response time, and higher sensitivity due to a decrease in diffusion length and an increase in accessible active sites.

Materials exhibit novel properties at nanometer dimension [49]. In the proposed sensor the novel properties of Cu-BTC nanoparticles had also a great effect on the increasing of the device life-time, decreasing of the device fabricating cost, and the miniaturization of sensor devices. Decreasing the size of Cu-BTC to nanoscale resulted in having stable suspension of Cu-BTC nanoparticles in ethanol for several hours, having homogenous droplet and also proper adhesion of nanoparticles together and to the substrate. It may con-

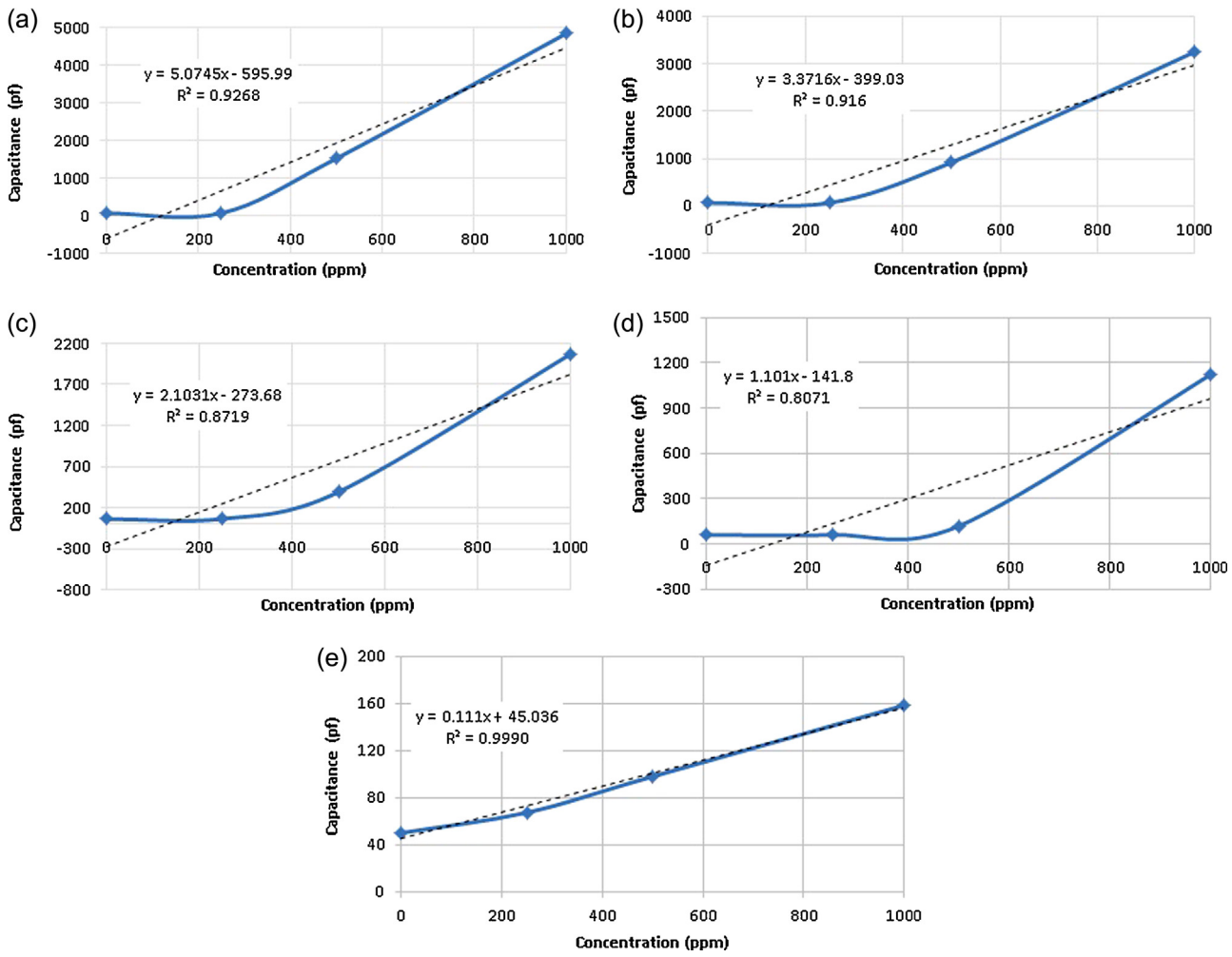

Fig. 6. The effect of LCR meter frequency on the capacitance changes of sensor *vs* methanol concentration of 250, 500 and 1000 ppm. The applied LCR meter frequency was fixed at (a) 800 Hz, (b) 1 Hz, (c) 1 kHz, (d) 100 kHz and (e) 1 MHz.

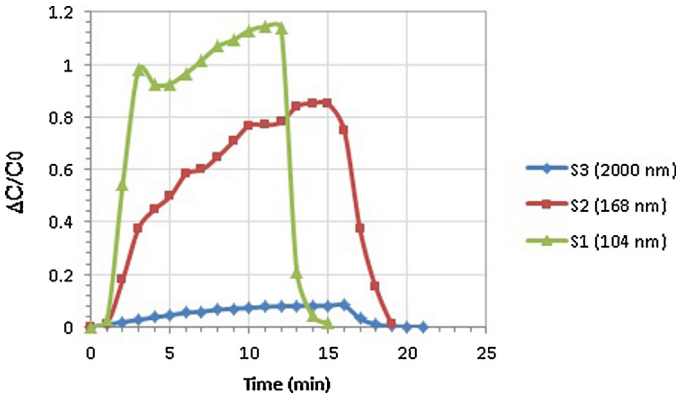

Fig. 7. The time-dependent capacitive responses of sensor with different Cu-BTC particle size of S1, S2 and S3 to 500 ppm ethanol at 25 °C and relative humidity of 10%.

sequently had effect on fabricating a uniform, dense and crack free layer with low cost drop casting method which lead to low capacitance leakage at alternating current and finally increasing of sensor life-time (Section 2.4). Therefore, in this work sensor S1 was chosen in all experiments.

3.2.2. *The effect of atmospheric humidity on sensor response*

To investigate the effect of relative humidity (RH) on the response of our system under the measurement condition, our system was exposed to atmospheric air during the days with different humidity levels. The humidity was measured by the commercial humidity sensor (available in our lab) in each day. In relative humidity of 5–30%, capacitance changes were negligible and but significant over 30%–50% (Fig. 8). Since at RH above 50%, Cu-BTC based capacitive sensor shows high humidity response, using of Cu-BTC based capacitive sensor is not suggested for the detection of VOCs above RH of 50%. Due to our limitation to control the humidity during the sensing process, we did our sensing test in the days when the relative humidity was about 10%.

3.2.3. *Reproducibility and reversibility measurements*

As mentioned above (Section 2.4), reproducibility of the sensor was investigated by fabricating four individual sensors. The results were shown in Table 3. A good reproducibility was obtained for four sensors (all standard deviation values in Table 3 were calculated for five repetitions of experiments).

To eliminate the possible influence of the sequence of the gas exposure as well as to verify the reliability of the recorded data, the samples were exposed to methanol followed by ethanol, isopropanol and acetone, and again in this manner for several times, for capacitive sensor measurements. These cycles were repeated seven times at ambient conditions with relative humidity about

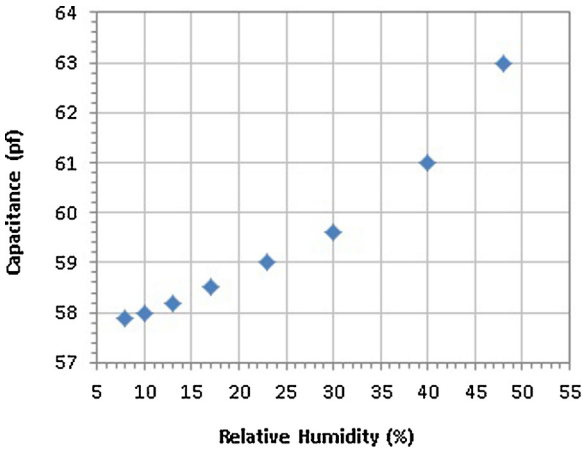

Fig. 8. Capacitive response of the Cu-BTC-based capacitive sensor to various relative humidity at 25 °C.

Table 3
Investigation of reproducibility of the sensor for methanol vapor at different concentration.

Concentration (ppm)	ΔC (pf)
250	37.7 ± 2.1
500	77.4 ± 3.3
1000	160.3 ± 4.0
1500	246.4 ± 4.3

10%, and the amount of sensor's capacitance changes was evaluated (Fig. 2S, Supporting information). Fig. 9 displays only two first cycles of these measurements for all target gases at different concentrations (250, 500, 1000 and 1500 ppm). Fig. 9 shows the device performance does not depend on exposing to different analytes. It means that for each target gas, the same capacitance changes pattern is observable during seven cycles regardless of exposing to different analytes sequentially. It indicates the precision and reliability of the device and its ability to provide reproducible results. In addition, in all experiments, the capacitance reached a platue while subjecting to each analyte vapors. Reversibility of the sensor was checked by exposing the sensor onto the atmosphere without

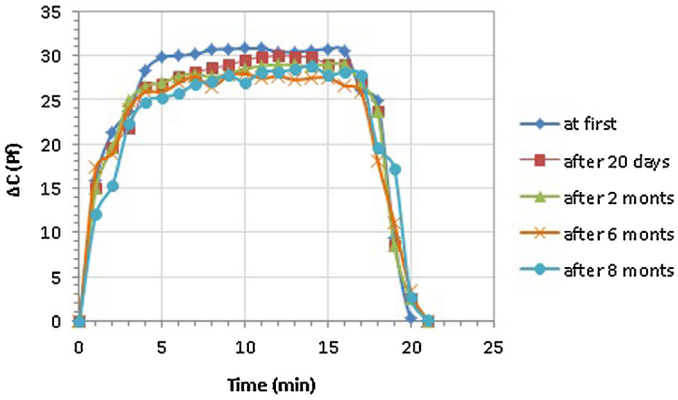

Fig. 10. Sensor performance or the time-dependent capacitive changes responses (ΔC) to 500 ppm methanol during 8 months.

heating. A rapid decrease of the capacitance into its original value proved that our sensor is very reversible.

Aging of the Cu-BTC framework was also observed during 8 months. As demonstrated in literatures [19,23], device performance was decreased during this period of time. But by heating for few minutes, we can treat this effect. Therefore, overlapping of different data sets collected over this period of time suggested retention of the device and its ability to provide reproducible results (Fig. 10). In addition, we did not find significant changes in the XRD patterns and IR spectra of Cu-BTC layer after exposing to analytes (see Fig. 3S, Supporting Information). FTIR spectra did not show any considerable changes before and after exposing to VOCs. In the case of XRD spectra, an increase in the peak intensity (no spectral shifts) was observed which is most likely resulted from the analytes uptake in the Cu-BTC pores [23,59,60]. Therefore, Cu-BTC structure showed a good stability after exposing to VOCs.

3.2.4. *Response time & recovery time*

Adsorption of a target vapor molecules alter the permittivity of the Cu-BTC layer, and; thereby, changes the capacitance of the elements in the array (Section 2.7). The sensor was exposed to each analyte vapor until the capacitance variations of the sensor reached a plateau in the time dependent response (steady-state response level). Afterwards, to recover the sensor, it was exposed into the

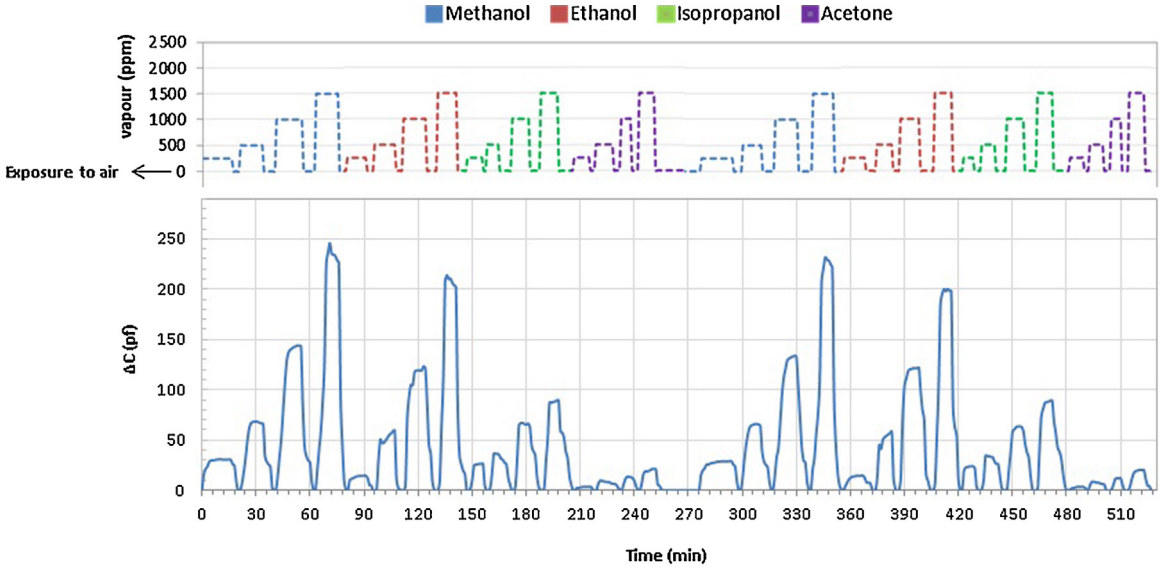

Fig. 9. The first two sensing-recovery cycles of the capacitive gas sensor measurements of methanol, ethanol, isopropanol, and acetone as target gases with concentration of 250, 500, 1000 and 1500 ppm at ambient condition with relative humidity below 20%.

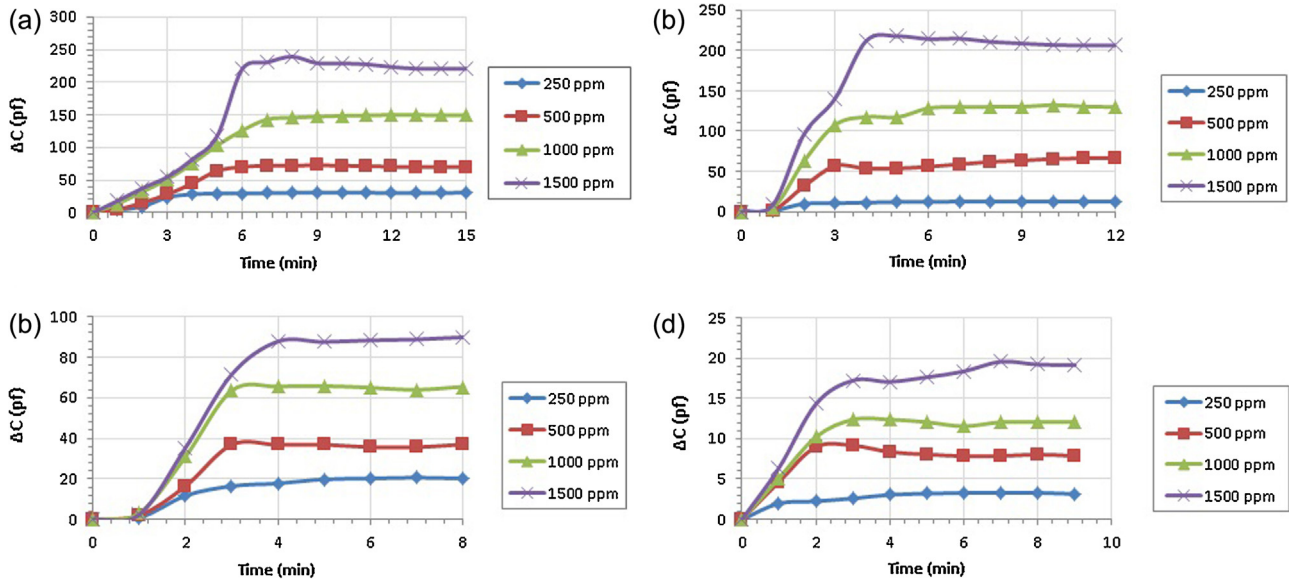

Fig. 11. Real-time capacitive Response of the Cu-BTC-based sensor after exposure to vapor of (a) methanol, (b) ethanol, (c) isopropanol and (d) acetone for different concentration of 250, 500, 1000 and 1500 ppm at ambient condition with relative humidity below 20%.

atmosphere until its capacitance value reached into its baseline (C_0) and in this step, the sensor was used again for next sensing cycle. The exposure time to target gases and the time allowed the sensor to recover to the baseline are various for different gases at different concentrations.

Fig. 11 shows that the real-time evolution of the capacitance changes after different concentration (250–1500 ppm) of analyte exposure. It has been observed that the sensor typically response within a second but frequently requires 2–6 min to reach equilibrium. In the sensor industries, the response time usually is measured in terms of the time for the sensor response to change from 10% to 90% of its projected steady-state response level upon analyte exposure [61]. And the recovery time is usually specified as time to fall to 10% of steady state value after the removal of the measured gas [62]. As we can see in Fig. 12, response time and recovery time depends on the type and concentration of target gases and for each analyte, they are increased by increasing the concentration.

3.2.5. Sensitivity

The sensitivity of the sensor for each concentration must be characterized by the relative percentage change in the response magnitude from baseline [63,64]. The method used for calculating the sensitivity was explained in supporting information (Section 3). Our sensor showed different sensitivities for various vapors in different concentrations. The most sensitivity was achieved for methanol, followed by ethanol, isopropanol, and acetone at ambient condition (at room temperature & humidity levels about 10%). These observations can be visually confirmed by referring to Fig. 13. The magnitude of sensitivity for each analyte variations of the sensor (Eq. (4), supporting information, Section 3). As demonstrated in Section 2.7, because of the rigidity of nanoporous Cu-BTC film, variations in capacitance of the sensor by exposing to analytes is only related to the change in dielectric constant of the dielectric material not to other effective parameters of the sensor such as A and d (Eq. (1)). Before subjecting the sensor to analytes, the nanopores of the Cu-BTC are occupied with atmospheric air. The capacitance value is increased after subjecting the sensor to polar analytes (with higher dielectric constant (Table 1)), because the Cu-BTC nanopores were occupied with analytes [51]. More adsorption of an analyte into the Cu-BTC layer with higher dielectric constant causes more capacitance changes and consequently more sensitivity of the sensor. Therefore, the magnitude of capacitance changes (ΔC) of our sensor for each analyte depends on a combination of different phenomenon such as the dielectric constant value of the analytes, their concentration, and the amount of their adsorption tendency onto the Cu-BTC layer.

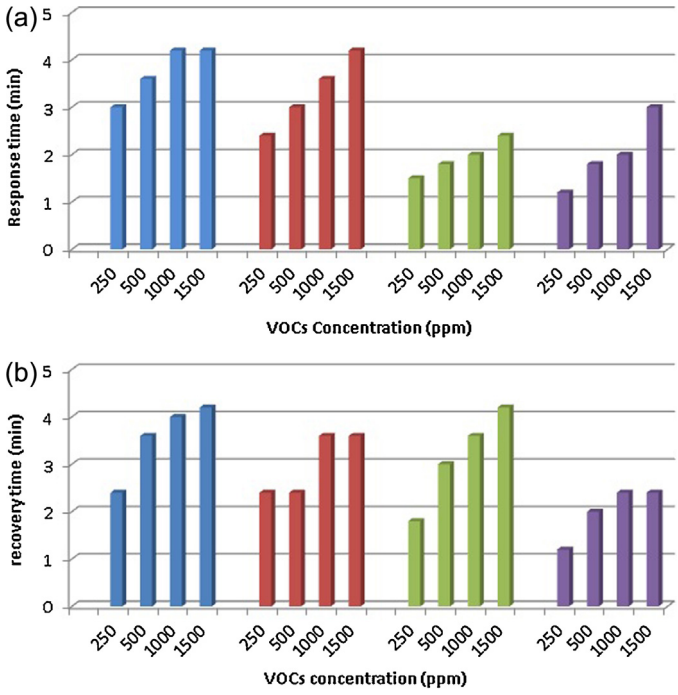

Fig. 12. (a) Response time and (b) Recovery time of the capacitive sensor versus different concentration on methanol, ethanol, isopropanol and acetone.

There are some unsaturated metal sites in Cu-BTC structure. According to the literature, when Cu-BTC layer was exposed to polar or polarizable molecules such as methanol or ethanol, these molecules preferentially coordinate to the copper ions of Cu-BTC where van der Waals interactions with Cu-BTC are maximized [69]. On the other hand, number of adsorbed alcohol molecules depends directly on the length of the alcohol chain (which depends on the number of carbon atoms, C_1–C_3), mass, and geometry as well as

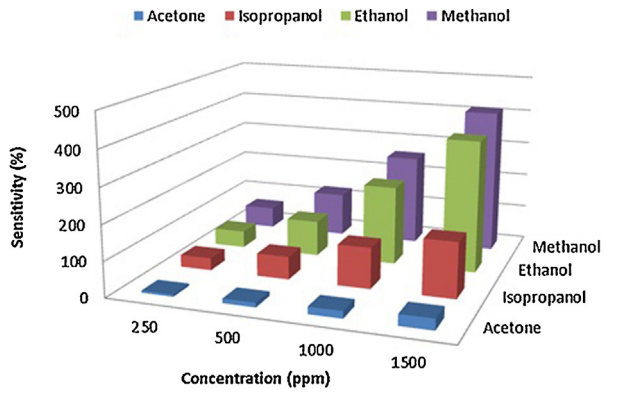

	250	500	1000	1500
Acetone	6.3	12.5	20.4	28.1
Isopropanol	35	65	116	157
Ethanol	48.6	101.5	224.7	375.8
Methanol	61	125.3	258.5	412.5

Fig. 13. Sensor sensitivity for methanol, ethanol, isopropanol and acetone at different concentration of 250, 500, 1000 and 1500 ppm.

polarity and kinetic diameter of these components. As demonstrated in literatures, number of adsorbed alcohol molecules in Cu-BTC layer is decreased by increasing chain length, mass, and size and increased by increasing polarity in dry atmosphere. Hence, as seen in Fig. 13, our sensor has the most sensitivity for methanol because methanol has the most dielectric constant and consequently the most adsorption tendency occurred onto the Cu-BTC layer due to its lowest chain length, lowest kinetic diameter, and lowest mass. However, in general, adsorption is a complicated phenomenon which is not well understood, thus above generalizations are not always the case. For example, isopropanol and acetone have similar kinetic diameters though dipole moment and dielectric constant of acetone is more than the dipole moment and dielectric constant of isopropanol. Therefore, the adsorption of isopropanol and in turn its sensitivity is higher than acetone (Table 1). It is also in agreement with [14], which reports about the Cu-BTC microcantilever sensor's response exposed to the different volatile organic compounds (VOCs) including acetone, isopropanol, methanol and water at different concentrations. Moreover, at low humidity levels (below 20%), our result is in agreement with the recent work by Davydovskaya et al. [23] for QCM sensor which was used for methanol, ethanol, 1-propanol, and isopropanol detection.

3.2.6. Linearity evaluation and limits of detection (LOD)

The response of the sensor towards different concentration of methanol, ethanol, isopropanol and acetone show a good linear relationship for the entire of range of the concentration shown in Fig. 14. According to the calibration curves for our data, we computed LOD values for ethanol, methanol, isopropanol, and acetone detection (Supporting information, section 4) [70]. In this manner, our measurements indicate the calculated LOD values of 61.99 ppm, 71.05 ppm, 77.80 and 100.18 ppm for methanol, ethanol, isopropanol, and acetone, respectively. Hence, Cu-BTC capacitive sensor provides a large dynamic range of response with capability to measure a few ppm to much higher values with high resolution.

3.2.7. Selectivity

To evaluate the selectivity of the sensor to polar or non-polar analyte vapors, various concentrations of *n*-hexane and toluene (250, 500, 1000, and 1500) were introduced to the sensor chamber. The characteristic responses are shown in Fig. 15. The sensing behavior is completely opposite to the behavior of the polar analytes. *N*-hexane and toluene produce a decrease in capacitance value upon exposure to the sensor surface. This decreasing in capacitance values can be related to the substitution of atmospheric water molecules which have been already occupied in the Cu-BTC nanopores by *n*-hexane and toluene molecules [51]. Because their dielectric constant is lower than water, capacitance of the sensor decreases by entering *n*-hexane and toluene molecules into the pores.

4. Conclusions

To the best of our knowledge, the present study is the first report on using of Cu-BTC particles in nanoscale for fabricating capacitive sensor for VOCs sensing. Thin films of Cu-BTC nanoparticles were investigated as dielectric layer of capacitive sensor for detection of different concentrations of methanol, ethanol, isopropanol, and acetone at ambient condition. Our results show that these analytes can be successfully detected with high sensitivity at ppm concentration levels (250–1500 ppm). The characteristic evaluation of the sensor peformance indicates that the sensor has good and reasonable response times, good linearity and reversible response at different concentrations. Moreover, different sensing behavior was observed towards methanol, ethanal, isopropanal, and acetone, depending on the dielectric constant, ambient concentration of the VOC, and the amount of their adsorption into the Cu-BTC film. The minimum detectable concentrations for sensing of methanol,

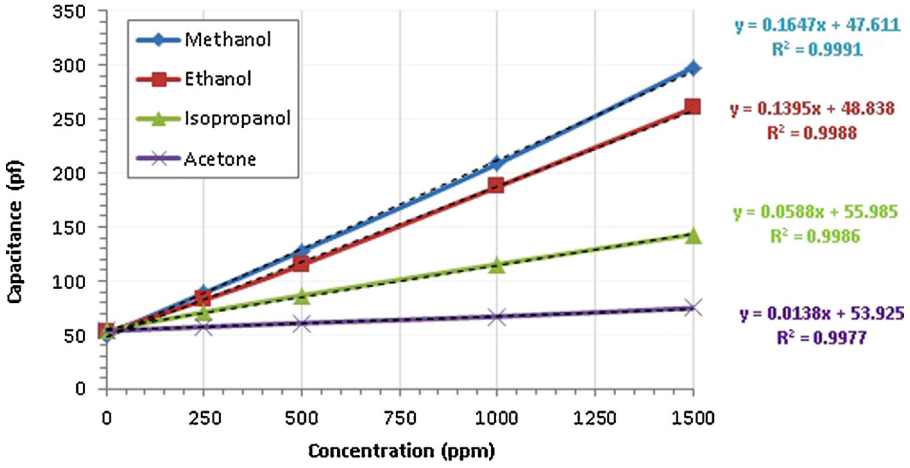

Fig. 14. Calibration curves the sensors for methanol, ethanol, isopropanol and acetone at the concentration range of 250, 500, 1000 and 1500 ppm.

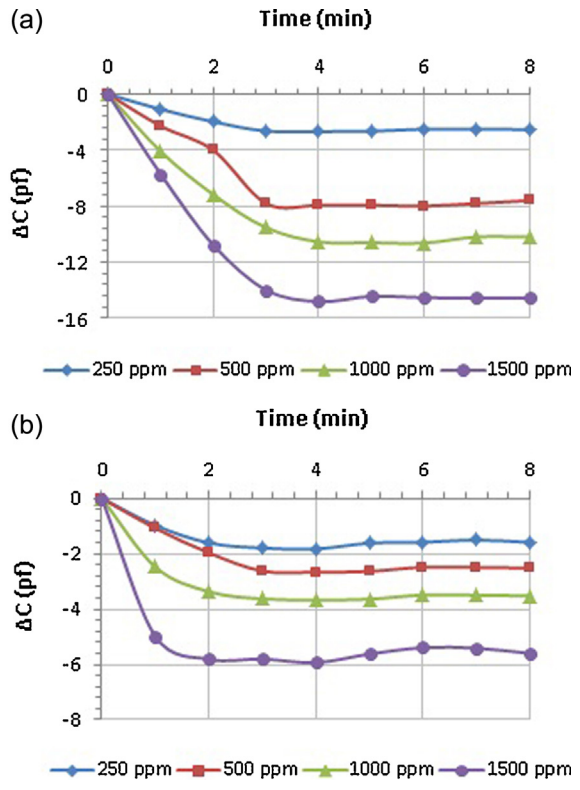

Fig. 15. Real time capacitive changes (ΔC) Cu-BTC-based capacitive sensor after exposer to 250, 500, 1000 and 1500 ppm of (a) *n*-Hexane (b) toluene.

ethanol, isopropanol, and acetone by this sensor are 61.99 ppm, 71.05 ppm, 77.80, and 100.18 ppm, respectively. To study the selectivity of proposed sensor, the surface was exposed to both polar and non-polar analytes which shows a proper selectivity for polar analytes.

Acknowledgment

We acknowledge the Nanotechnology Research Institute of Shiraz University and the Iran Ministry of Science and Technology as providers of financial sum, facilities, contributors, etc.

Appendix A. Supplementary data

Supplementary data associated with this article can be found, in the online version, at http://dx.doi.org/10.1016/j.snb.2016.06.152.

References

[1] M. Madou, S. Morrison, Chemical Sensing with Solid State Devices, Academic Press Inc., San Diego, 1989.
[2] H. Bai, G. Shi, Gas sensors based on conducting polymers, Sensors 7 (2007) 267–307.
[3] J.M. Slater, E.J. Watt, N.J. Freeman, I.P. May, D.J. Weir, Gas and vapor detection with poly (pyrrole) gas sensors, Analyst 117 (1992) 1265–1270.
[4] G. Aggazzotti, G. Fantuzzi, E. Righi, G. Predieri, Blood and breath analyses as biological indicators of exposure to trihalomethanes in indoor swimming pools, Sci. Total Environ. 217 (1998) 155–163.
[5] M.D. Allendorf, A. Schwartzberg, V. Stavila, A.A. Talin, A roadmap to implementing metal–organic frameworks in electronic devices: challenges and critical directions, Chem. Eur. J. 17 (2011) 11372–11388.
[6] A.J. Fletcher, K.M. Thomas, M.J. Rosseinsky, Flexibility in metal–organic framework materials: impact on sorption properties, J. Solid State Chem. 178 (2005) 2491–2510.
[7] K. Uemura, R. Matsuda, S. Kitagawa, Flexible microporous coordination polymers, J. Solid State Chem. 178 (2005) 2420–2429.
[8] J.-R. Li, R.J. Kuppler, H.-C. Zhou, Selective gas adsorption and separation in metal–organic frameworks, Chem. Soc. Rev. 38 (2009) 1477–1504.
[9] A.L. Robinson, V. Stavila, T.R. Zeitler, M.I. White, S.M. Thornberg, J.A. Greathouse, M.D. Allendorf, Ultrasensitive humidity detection using metal–organic framework-coated microsensors, Anal. Chem. 84 (2012) 7043–7051.
[10] A.H. Khoshaman, B. Bahreyni, Application of metal organic framework crystals for sensing of volatile organic gases, Sens. Actuators B 162 (2012) 114–119.
[11] H. Yamagiwa, S. Sato, T. Fukawa, T. Ikehara, R. Maeda, T. Mihara, M. Kimura1, Detection of volatile organic compounds by weight-detectable sensors coated with metal–organic frameworks, Sci. Rep. 4 (2014) 6247.
[12] A. Venkatasubramanian, J.-H. Lee, R.J. Houk, M.D. Allendorf, S. Nair, P.J. Heskethe, Characterization of HKUST-1 crystals and their application to MEMS microcantilever array sensors, ECS Trans. 33 (2010) 229–238.
[13] M.D. Allendorf, R.J.T. Houk, L. Andruszkiewicz, A.A. Talin, J. Pikarsky, A. Choudhury, K.A. Gall, P.J. Hesketh, Stress-induced chemical detection using flexible metal–organic frameworks, J. Am. Chem. Soc. 130 (2008) 14404–14405.
[14] I. Ellern, A. Venkatasubramanian, J.H. Lee, P.J. Hesketh, V. Stavilla, M.D. Allendorf, A.L. Robinson, Characterization of piezoresistive microcantilever sensors with metal organic frameworks for the detection of volatile organic compounds, ECS Trans. 12 (2013) 469–476.
[15] J. Liu, F. Sun, F. Zhang, Z. Wang, R. Zhang, C. Wangb, S. Qiu, In situ growth of continuous thin metal–organic framework film for capacitive humidity sensing, J. Mater. Chem. 21 (2011) 3775–3778.
[16] G. Hagen, J. Kita, M. Itamar, M.S. Achmann, C. Kiener, R. Moos, Metal–organic frameworks for sensing applications in the gas phase, Sensors 9 (2009) 1574–1589.
[17] T. Terencio, F. Di Renzo, D. Berthomieu, P. Trens, Adsorption of acetone vapor by Cu-BTC: an experimental and computational study, J. Phys. Chem. C 117 (2013) 26156–26165.
[18] P. Kusgens, M. Rose, I. Senkovska, H. Frode, A. Henschel, S. Siegle, S. Kaskel, Characterization of metal–organic frameworks by water adsorption, Microporous Mesoporous Mater. 120 (2009) 325–330.
[19] T. Van Assche, T. Duerinck, J.J. Gutierrez Sevillano, S. Calero, G.V. Baron, J.F.M. Denayer, High adsorption capacities and two-step adsorption of polar adsorbates on copper-benzene-1,3,5-tricarboxylate metal–organic framework, J. Phys. Chem. C 117 (2013) 18100–18111.
[20] A. Poppl, B. Jee, M. Icker, M. Hartmann, D. Himsl, Untersuchungen zur chemischen stabilität von cu3(btc)2 (HKUST-1) durch N2-adsorption, röntgenpulverdiffraktometrie und EPR-spektroskopie, Chem. Ing. Tech. 82 (2010) 1025–1029.
[21] P.M. Schoenecker, H.J. Jasuja, C.G. Carson, H. Jasuja, C.J. Flemming, K.S. Walton, Effect of water adsorption on retention of structure and surface area in metal–organic frameworks, Ind. Eng. Chem. Res. 51 (2012) 6513–6519.
[22] K.A. Cychosz, A.J. Matzger, Water stability of microporous coordination polymers and the adsorption of pharmaceuticals from Water, Langmuir 26 (2010) 17198–17202.
[23] P. Davydovskaya, A. Ranft, B.V. Lotsch, R. Pohle, Analyte detection with Cu-BTC metal–organic framework thin films by means of mass-sensitive and work-function-based readout, Anal. Chem. 86 (2014) 6948–6958.
[24] T. Ishihara, S. Sato, T. Fukushima, Y. Takita, Capacitive gas sensor of mixed oxide CoO-1n_2O_3 to selectively detect nitrogen monoxide, J. Electrochem. Soc. 143 (1996).
[25] T. Ishihara, S. Matsubara, Capacitive type gas sensors, J. Electroceram. 2 (4) (1998) 215–228.
[26] W.P. Tai, J.H. Oh, Preparation and humidity sensing behaviors of nanocrystalline SnO_2/TiO_2 bilayered films, Thin Solid Films 1-2 (2002) 220–224.
[27] C. Cantalini, L. Valentini, I. Armentano, L. Lozzi, J.M. Kenny, S. Santucci, Sensitivity to NO_2 and cross-sensitivity analysis to NH_3, ethanol and humidity of carbon nanotubes thin film, in: M.C. Glenn, J.A., Schuetz (Eds.), An IC Compatible Polymer Humidity Sensor, Technology Digest, Transducers'85, Philadelphia, PA, USA, 1985 217–220.
[28] Y.F. Qiu, S.H. Yang, ZnO nanotetrapods: controlled vapor-phase synthesis and application for humidity sensing, Adv. Funct. Mater. 17 (2007) 1345–1352.
[29] M. Shafiei, R. Arsat, J. Yu, K. Kalantar-zadeh, W. Wlodarski, Pt/graphene nano-sheets based hydrogen sensor, Proc. IEEE Sens. (2009) 295–298.
[30] J. Yua, H. Wen, M. Shafiei, M.R. Field, Z.F. Liu, W. Wlodarski, N. Motta, Y.X. Li, K. Kalantar-zadeh, P.T. Lai, A hydrogen/methane sensor based on niobium tungsten oxide nanorods synthesized by hydrothermal method, Sens. Actuators B 184 (2013) 118–129.
[31] C. Piloto, F. Mirri, E.A. Bengio, M. Notarianni, B. Gupta, M. Shafiei, M. Pasquali, N. Motta, Room temperature gas sensing properties of ultrathin carbon nanotubes by surfactant-free dip coating, Sens. Actuators B 227 (2016) 128–134.
[32] Y. Sakata, S. Furukawa, M. Kondo, K. Hirai, N. Horike, Y. Takashima, H. Uehara, N. Louvain, M. Meilikhov, T. Tsuruoka, S. Isoda, W. Kosaka, O. Sakata, S. Kitagawa, Shape-memory nanopores induced in coordination frameworks by crystal downsizing, Science 339 (2013) 193–196.
[33] D. Tanaka, A. Henke, K. Albrecht, M. Moeller, K. Nakagawa, S. Kitagawa, J. Groll, Rapid preparation of flexible porous coordination polymer nanocrystals with accelerated guest adsorption kinetics, Nat. Chem. 2 (2010) 410–416.
[34] G. Bussetti, S. Trabattoni, S. Uttiyab, A. Sassellab, M. Rivaa, A. Piconea, A. Brambillaa, L. Duòa, F. Ciccacci, M. Finazzi, Controlling drop-casting deposition of 2D Pt-octaethyl porphyrin layers on graphite, Synth. Met. 195 (2014) 201–207.

[35] J. Perelaer, P.J. Smith, M.M.P. Wijnen, E. van den Bosch, R. Eckardt, P.H.J.M. Ketelaars, U.S. Schubert, Droplet tailoring using evaporative inkjet printing, Macromol. Chem. Phys. 210 (2009) 387–393.
[36] C.S. Kim, S. Lee, E.D. Gomez, J.E. Anthony, Y.-L. Loo, Solvent-dependent electrical characteristics and stability of organic thin-film transistors with drop cast bis (triisopropylsilylethynyl) pentacene, Appl. Phys. Lett. 93 (2008) 103302.
[37] N. Patra, M. Salerno, A. Diaspro, A. Athanassiou, Effect of solvents on the dynamic viscoelastic behavior of poly(methyl methacrylate) film prepared by solvent casting, J. Mater. Sci. 46 (2011) 5044–5049.
[38] R.V. Hameren, A.M. van Buul, M.A. Castriciano, V. Villari, N. Micali, P. Schon, S. Speller, L.M. Scolaro, A.E. Rowan, J.A.A.W. Elemans, R.J.M. Nolte, Supramolecular porphyrin polymers in solution and at the solid-liquid interface, Nano Lett. 8 (2008) 253–259.
[39] J. Park, S. Lee, H.H. Lee, High-mobility polymer thin-film transistors fabricated by solvent-assisted drop-casting, Org. Electron. 7 (2006) 256.
[40] R. Meinhardt, S. Macko, B. Qi, A. Draude, Y. Zaho, W. Wenig, H. Franke, Photoinduced molecular motion in an azobenzene-containing diblock copolymer, J. Phys. D: Appl. Phys. 41 (2008) 195303.
[41] K.A. Singh, T. Young, R.D. McCullough, T. Kowalewski, L.M. Porter, Planarization of polymeric field-Effect transistors: improvement of nanomorphology and enhancement of electrical performance, Adv. Funct. Mater. 20 (2010) 2216–2221.
[42] C. Zhao, L. Xinga, J. Xiang, L. Cui, J. Jiaoc, H. Sai, Z. Li, F. Li, Formation of uniform reduced graphene oxide films on modified PET substrates using drop-casting method, Particuology 17 (2014) 66–73.
[43] H. Ko, V. Tsukruk, Liquid-crystalline processing of highly oriented carbon nanotube arrays for thin-film transistors, Nano Lett. 6 (2006) 1443–1448 (Featured in SPIE newsroom, Solution Processing Simplifies the Manufacturing of Carbon Nanotube Transistors, 2006, x8606).
[44] M.C. Glenn, J.A. Schuetz, An IC compatible polymer humidity sensor, technology digest, in: Transducers'85, Philadelphia, PA, USA, 1985, pp. 217–220.
[45] G. Delapierre, H. Grange, B. Chambaz, L. Destannes, Polymer-based capacitive humidity sensor: characteristics and experimental results, Sens. Actuators B Chem. 4 (1983) 97–104.
[46] H. Shibata, M. Ito, M. Asakursa, K. Watanabe, A digital hygrometer using a polyimide film relative humidity sensor, IEEE Trans. Instrum. Meas. 45 (2) (1996) 564–569.
[47] E. Fotis, A new ammonia detector based on thin film polymer technology, Sensors 19 (5) (2002) 73–75.
[48] D.D. Denton, S.D. Senturia, E.S. Anolick, D. Scheider, Fundamental issues in the design of polymeric capacitive moisture sensors, technical digest, in: Transducers'85, Philadelphia, PA, USA, 1985, pp. 202–205.
[49] S. Mintova, M. Jaber, V. Valtcheva, Nanosized microporous crystals: emerging applications, Chem. Soc. Rev. 44 (2015) 7207–7233.
[50] F. Hossein-babaei, A. Amini, A breakthrough in gas diagnosis with a temperature-modulated generic metaloxide gas sensor, Sens. Actuators B 166–167 (2012) 419–425.
[51] M.S. Hosseini, S. Zeinali, M.H. Sheikhi, Fabrication of capacitive sensor based on Cu-BTC (MOF-199) nanoporous film for detection of ethanol and methanol vapors, Sens. Actuators B 230 (2016) 9–16.
[52] E. Biemmi, C. Scherb, T. Bein, Oriented growth of the metal organic framework $Cu_3(BTC)_2(H2O)_3$ xH_2O tunable with functionalized self-assembled momolayers, J. Am. Chem. Soc. 129 (2007) 8054–8055.
[53] F. Wang, H. Guo, Y. Chai, Y. Li, C. Liu, The controlled regulation of morphology and size of HKUST-1 by "coordination modulation method", Microporous Mesoporous Mater. 173 (2013) 181–188.
[54] E. Biemmi, A. Darga, N. Stock, T. Bein, Direct growth of Cu3(BTC)2(H2O)3. xH2O thin films on modified QCM-gold electrodes – water sorption isotherms, Microporous Mesoporous Mater. 114 (2008) 380–386.
[55] Y. Wang, Y. Wu, J. Xie, H. Ge, X. Hu, Multi-walled carbon nanotubes and metal–organic framework nanocomposites as novel hybrid electrode materials for the determination of nano-molar levels of lead in a lab-on-valve format, Analyst 138 (2013) 5113–5120.
[56] Z.-Q. Li, L.-G. Qiu, T. Xu, Y. Wu, W. Wang, Z.-Y. Wu, X. Jiang, Ultrasonic synthesis of the microporous metal–organic framework $Cu_3(BTC)2$ at ambient temperature and pressure: an efficient and environmentally friendly method, Mater. Lett. 63 (2009) 78–80.
[57] X. Ming Liu, S.u Rather, Q. Li, A. Lueking, Y. Zhao, J. Li, Hydrogenation of CuBTC framework with the introduction of a PtC hydrogen spillover catalyst, J. Phys. Chem. C 116 (2012) 3477–3485.
[58] T. Brock, M. Groteklaes, P. Mischke, European Coatings Handbook, Th, Schafer, Hannover, Germany, 2000.
[59] E. Borfecchia, S. Maurelli, D. Gianolio, E. Groppo, M. Chiesa, F. Bonino, C. Lamberti, Insights into adsorption of NH3 on HKUST-1 metal–organic framework: a multitechnique approach, J. Phys. Chem. C 116 (2012) 19839–19850.
[60] J. Hafizovic, M. Bjørgen, U. Olsbye, P.D.C. Dietzel, S. Bordiga, C. Prestipino, C. Lamberti, K.P. Lillerud, The inconsistency in adsorption properties and powder XRD data of MOF-5 is rationalized by framework interpenetration and the presence of organic and inorganic species in the nanocavities, J. Am. Chem. Soc. 129 (2007) 3612–3620.
[61] K.M.E. Stewart, A. Penlidis, Novel test system for gas sensing materials and sensors, macromolecular symposia, Polym. React. Eng. 324 (2013) 11–18, VIII.
[62] S.M. Sze, Semiconductor Sensors, John Wiley & Sons, Inc., New York, 1994.
[63] J.J. Carr, J.M. Brown, Sensor Terminology, Introduction to Biomedical Equipment Technology, third ed., National Instruments & Prentice Hall, 2010, 2016.
[64] S. Achmann, G. Hagen, J. Kita, I.M. Malkowsky, C. Kiener, R. Moos, Metal–organic frameworks for sensing applications in the gas phase, Sensors 9 (2009) 1574–1589.
[65] Abbott, Steven and Hansen, Charles M., Hansen Solubility Parameters in Practice (2008) ISBN 0–9551220-2-3.
[66] https://en.wikipedia.org/wiki/Solvent.
[67] T. Borjigin, F. Sun, J. Zhang, K. Cai, H. Rena, G. Zhu, A microporous metal–organic framework with high stability for GC separation of alcohols from water, Chem. Commun. 48 (2012) 7613–7615.
[68] L. Gales, A. Mendes, C. Costa, Hysteresis in the cyclic adsorption of acetone, ethanol and ethyl acetate on activated carbon, Carbon 38 (2000) 1083–1088.
[69] C. Chmelik, J. Karger, M. Wiebcke, J. Caro, J.M. van Baten, R. Krishna, Adsorption and diffusion of alkanes in CuBTC crystals investigated using infra-Red microscopy and molecular simulations, Microporous Mesoporous Mater. 117 (2009) 22–32.
[70] J.N. Miller, J.C. Miller, Statis Tics and Chemometrics for Analytical Chemistry, fifth ed., Pearson Education, Canada, 2005.

Biographies

Setare Homayoonnia received her BSc in Chemical engineering in 2008 from University of Sistan and Baluchestan and her MSc in Nanochemical Engineering under the supervision of Dr. Sedigheh Zeinali, in 2015, from Shiraz University, Iran. Her previous research is focused on Design and Fabrication of solar desalination system and her current research is focused on the nanoMOF and MOF nanocomposite synthesis and fabricating their thin layer through drop casting methods in order to fabricate capacitive and resistive sensors.

Sedigheh Zeinali studied chemistry and received her BSc in chemistry from Shiraz University, in 1999 and MSc in analytical chemistry from Zanjan University, in 2002. She received her PHD in analytical chemistry under supervision of Prof. Afsaneh Safavi from Department of Chemistry at Shiraz University in 2010. She is currently assistant professor in Nanochemical Engineering Department, faculty of advanced technologies, Shiraz University, Iran. Her current research is focused on the synthesis of different kinds of MOFs and their application in fabrication of capacitive gas sensors. She is also studies and researches on the application of MOFs in the adsorption and removal of organic and inorganic pollutants from air and water.